

pH-Dependent Excited-State Dynamics of $[\text{Ru}(\text{bpy})_3]^{2+}$ -Modified Amino Acids: Effects of an Amide Linkage and Remote Functional Groups[†]

Bernd Geisser,[‡] Adrian Ponce,[§] and Ralf Alfsasser^{*,‡}

Institute for Inorganic Chemistry, University of Erlangen-Nürnberg, Egerlandstr. 1, 91058 Erlangen, Germany, and Beckman Institute, California Institute of Technology, Pasadena, California 91125

Received July 28, 1998

The pH-dependent photophysical properties of a series of polypyridyl ruthenium-substituted amino acids were investigated by steady-state and time-resolved luminescence spectroscopy. $[\text{H}_3\text{N}-\text{DAPA}(\text{Rub}_2\text{m})-\text{OH}](\text{PF}_6)_3$ (**1**), $[\text{H}_3\text{N}-\text{DABA}(\text{Rub}_2\text{m})-\text{OH}](\text{PF}_6)_3$ (**2**), $[\text{H}_3\text{N}-\text{Orn}(\text{Rub}_2\text{m})-\text{OH}](\text{PF}_6)_3$ (**3**), and $[\text{H}_3\text{N}-\text{Lys}(\text{Rub}_2\text{m})-\text{OH}](\text{PF}_6)_3$ (**4**) were obtained by formation of an amide link between the ω - NH_2 group of the respective commercially available amino acid and $[\text{Rub}_2(\text{m}-\text{OH})]^{2+}$ (b = bipyridine, m-OH = 4'-methyl-2,2'-bipyridine-4-carboxylic acid). Due to the absence of significant electronic interactions between the ruthenium chromophore and the amino acid moieties, the energetics and extinction coefficients of the absorption spectra of **1–4** do not change as a function of pH. The luminescence intensities of these complexes, however, show a marked dependence on pH. At low pH (<2), quenching via excited-state protonation of the amide link leads to short lifetimes. In the pH 2–8 range, the lifetimes depend on the amino acid side chain length of the complex. At high pH (>9), lifetimes are approaching that of $[\text{Ru}(\text{bpy})_3]^{2+}$, suggesting that the amino acid moiety has a negligible effect on nonadiabatic pathways in the excited-state decay of the ruthenium moiety. Our results are discussed with respect to the rapidly growing interest in ruthenium-substituted amino acids as spectroscopic and mechanistic tools in biological systems.

Introduction

Because of their unique photophysical properties, polypyridyl ruthenium complexes find an increasing interest as luminescent structure/function sensors in the chemistry of biological macromolecules. Their use as spectroscopic and mechanistic probes for proteins¹ and DNA structures is well established.^{2,3} Recent developments involving proteins as target sites include the molecular recognition of $[\text{Ru}(\text{bpy})_3]^{2+}$ and $[\text{Ru}(\text{phen})_3]^{2+}$ derivatives by a monoclonal antibody⁴ and ruthenium modified proteins as anisotropy probes for solution dynamics and immunoassays of antigens.⁵ In the latter work, amino acid side chains have been selectively labeled with $[\text{Ru}(\text{bpy})_3]^{2+}$ units. This approach has also been successfully used for the construction of several redox active peptides⁶ and proteins.^{7–9} These examples illustrate the potential of modified metal binding

amino acids as powerful tools for structural and mechanistic studies in biologically relevant systems. A wide variety of possible further applications, such as labeling of transition metal pharmaceuticals via the amino acid functionality^{10,11} or probing substrate–surface interactions in peptid-modified monolayers,¹² may be envisioned.

A key feature of these applications is the change in photophysical properties of ruthenium chromophores on changing the microenvironment provided by biological macromolecules. It is therefore of fundamental interest to study the detailed mechanisms of the underlying phenomena in order to improve and fully exploit the wealth of information provided by emission spectroscopy. This has stimulated a number of studies dealing with medium effects such as changing solvent polarity^{13–15} or pH^{16,17} on the excited-state properties of polypyridyl ruthenium complexes.

Work in our laboratories focuses on the development of new synthetic amino acids with polydentate binding sites for transition metal centers as building blocks for biomimetic

* To whom correspondence should be addressed. Fax: 49-9131-8527387. E-mail: alfsassr@anorganik.chemie.uni-erlangen.de.

[†] Dedicated to Prof. O. J. Scherer on occasion of his 65th birthday.

[‡] University of Erlangen-Nürnberg.

[§] California Institute of Technology.

- (1) Gray, H. B.; Winkler, J. R. *Annu. Rev. Biochem.* **1996**, *65*, 537–561.
- (2) Barton, J. K. In *Bioinorganic Chemistry*; Bertini, I., Gray, H. B., Lippard, S. J., Valentine, J. S., Eds.; University Science Books: Mill Valley, 1994; pp 455–503.
- (3) Meade, T. J. In *Interactions of Metal Ions with Nucleotides, Nucleic Acids, and their Constituents*; Sigel, A., Sigel, H., Eds.; Marcel Dekker: New York, 1996; Vol. 32, pp 453–478.
- (4) Shreder, K.; Harriman, A.; Iverson, B. L. *J. Am. Chem. Soc.* **1996**, *118*, 3192–3201.
- (5) Szmackinski, H.; Terpetschnig, E.; Lakowicz, J. R. *Biophys. Chem.* **1996**, *62*, 109–120.
- (6) McCafferty, D. G.; Bishop, B. M.; Wall, C. G.; Hughes, S. G.; Mecklenburg, S. L.; Meyer, T. J.; Erickson, B. W. *Tetrahedron* **1995**, *51*, 1093–1106.
- (7) Durham, B.; Pan, L. P.; Long, J. E.; Millett, F. *Biochemistry* **1989**, *28*, 8659–8665.

- (8) Liu, R.-Q.; Miller, M. A.; Han, G. W.; Hahm, S.; Geren, L.; Hibdon, S.; Kraut, J.; Durham, B.; Millett, F. *Biochemistry* **1994**, *33*, 8678–8685.
- (9) Wuttke, D. S.; Gray, H. B.; Fisher, S. L.; Imperiali, B. *J. Am. Chem. Soc.* **1993**, *115*, 8455–8456.
- (10) Jurisson, S.; Berning, D.; Jia, W.; Ma, D. *Chem. Rev.* **1993**, *93*, 1137–1156.
- (11) Parker, D. *Chem. Soc. Rev.* **1990**, *19*, 271–291.
- (12) Cha, X.; Ariga, K.; Kunitake, T. *J. Am. Chem. Soc.* **1996**, *118*, 9545–9551.
- (13) Caspar, J. V.; Meyer, T. J. *J. Am. Chem. Soc.* **1983**, *105*, 5583–5590.
- (14) Sun, H.; Hoffman, M. Z. *J. Phys. Chem.* **1993**, *97*, 11956–11959.
- (15) Nair, R. B.; Cullum, B. M.; Murphy, C. J. *Inorg. Chem.* **1997**, *36*, 962–965.
- (16) Sun, H.; Hoffman, M. Z. *J. Phys. Chem.* **1993**, *97*, 5014–5018.
- (17) Cargill Thompson, A. M. W.; Smailes, M. C. C.; Jeffery, J. C.; Ward, M. D. *J. Chem. Soc., Dalton Trans.* **1997**, 737–743.

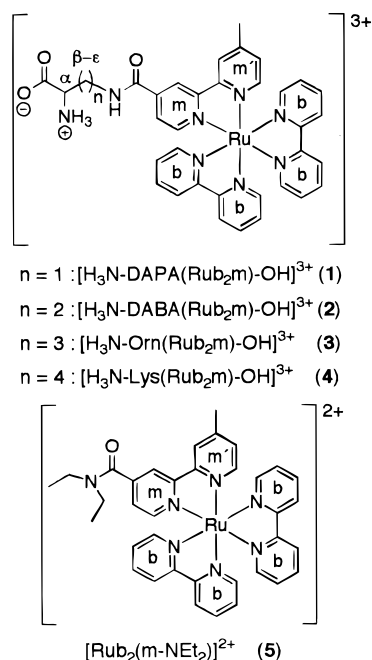


Figure 1. Structures and NMR labeling scheme of the ruthenium-substituted amino acids **1–4** and of the *N,N*-diethylamide **5**.

assemblies.^{18,19} Here, we report the synthesis and pH-dependent emission data of a series of $[\text{Ru}(\text{bpy})_3]$ -substituted amino acids (**1–4**, Figure 1). The aim of this study was to gain more insight into the basic structural features determining the photophysical properties of luminescent, photoredox-active building blocks for biological and biomimetic studies.

Our results demonstrate how the protonation of a remote amino acid group can significantly modify the photophysical properties of a chromophore linked to a biologically relevant molecule. Furthermore, the amide linkage used in our complexes is shown to play an important role in nonradiative decay pathways.

Experimental Section

Spectroscopy and CHN Analysis. UV–vis spectra were recorded on a Shimadzu UV-2101PC scanning spectrophotometer. Molar extinction coefficients were obtained from absorbance measurements as a function of complex concentration. IR spectra were recorded on a Mattson Polaris FT IR spectrophotometer using KBr pellets.

Proton NMR spectra were obtained on a Bruker Avance DPX 300 spectrometer. Solvent resonances were used as internal standards for measurements in methanol-*d*₄.

C, H, N elemental analyses were performed on a Carlo Erba Elemental Analyzer model 1106 at the analytical service station of this department.

Luminescence spectra were recorded on a Perkin-Elmer LS 50B spectrophotometer ($\lambda_{\text{exc}} = 450 \text{ nm}$, $\lambda_{\text{obs}} = 550\text{--}850 \text{ nm}$) equipped with a Hamamatsu R928 photomultiplier tube. $10 \mu\text{M}$ solutions of the complexes at different pH values were used, and the data were corrected for detector response.

Lifetimes. Luminescence lifetimes were obtained by exciting the samples with 480 nm light (20 ns fwhm, 2–3 mJ) obtained from a Lambda Physik FL 3002 dye laser (coumarin 480) pumped with a Lambda Physik LPX210i XeCl excimer laser. Shot selection was performed using a leading edge peak trigger directly linked to the digitizer. Single-wavelength kinetics were obtained by passing the emission from the sample through a 160B Instruments SA double monochromator and detecting the light with a Hamamatsu R928

Table 1. Experimental Details for the Synthesis of the $^{\alpha}\text{N}$ -Protected Amino Acids $^{\alpha}\text{N}$ -Boc-**1–4**

product	$[\text{Ru}_2(\text{m-OSu})](\text{PF}_6)_2$ g (mmol)	$^{\alpha}\text{N}$ -Boc-AA g (mmol)	yield ^a g (%)
$^{\alpha}\text{N}$ -Boc- 1	1.30 (1.30)	0.40 (1.95)	1.37 (94)
$^{\alpha}\text{N}$ -Boc- 2	1.40 (1.38)	0.45 (2.07)	1.35 (88)
$^{\alpha}\text{N}$ -Boc- 3	1.10 (1.00)	0.35 (1.50)	1.05 (92)
$^{\alpha}\text{N}$ -Boc- 4	1.40 (1.38)	0.51 (2.07)	1.44 (91)

^a Based on $[\text{Ru}_2(\text{m-OSu})](\text{PF}_6)_2$.

photomultiplier tube. The signal was fed first to a 200 MHz amplifier and then to a Tektronix RTD710A 200-MSs 10-bit transient digitizer interfaced to a PC.

Titration Curves. pH values were measured using a pH537 WTW Microprocessor pH meter equipped with an Ingold 402-M6-S7 Ag/AgCl reference electrode. Solutions of the complexes in Britton Robinson buffers²⁰ at 0.1 M ionic strength were used in a pH range from 1.8 to 12. Lower pH values were adjusted with calculated volumes of 2 or 12 M HCl, and higher pH values with 2 M NaOH, respectively. The final complex concentration was $10 \mu\text{M}$ in all cases. Emission titration curves were followed by uncorrected luminescence spectra obtained on the instrument described above ($\lambda_{\text{exc}} = 450 \text{ nm}$, $\lambda_{\text{obs}} = 550\text{--}850 \text{ nm}$).

Materials. RuCl_3 was a donation from Degussa. $[\text{Ru}(\text{bpy})_2\text{Cl}_2]^{2+}$ $[\text{Ru}(\text{bpy})_2(\text{m-OH})](\text{PF}_6)_2$,²² and $[\text{Ru}(\text{bpy})_2(\text{m-OSu})](\text{PF}_6)_2$ ($\text{m-OSu} = 4\text{-carboxysuccinimidoester-4'-methyl-2,2'-bipyridine}$)²² were prepared as described in the literature. $^{\alpha}\text{N}$ -Boc-protected amino acids were purchased from Bachem and used as received. Reagent grade solvents were obtained from Roth, NMR solvents and all other chemicals from Aldrich. DMF and acetonitrile were purified by distillation over CaH_2 under N_2 . Water for preparations and mechanistic studies was demineralized.

Protected Amino Acid Complexes. The $^{\alpha}\text{N}$ -Boc-protected amino acid complexes $[\text{Ru}(\text{bpy})_2(\text{m-OSu})\text{-OH}](\text{PF}_6)_2$ (AA = DAPA, DABA, Orn, Lys) were synthesized by coupling $[\text{Ru}(\text{bpy})_2(\text{m-OSu})](\text{PF}_6)_2$ with the respective amino acid according to the literature procedure reported for the lysine derivative $^{\alpha}\text{N}$ -Boc-**4**.²² Experimental quantities and respective yields are compiled in Table 1.

[Bis(2,2'-bipyridine)(4-(carboxamido- $^{\alpha}\text{N}$ -($^{\alpha}\text{N}$ -1,1-dimethylethoxy-carbonyl-L-2,3-diaminopropionic acid))-4'-methyl-2,2'-bipyridyl)-ruthenium(II)] Bis(hexafluorophosphate) [$^{\alpha}\text{N}$ -Boc-DAPA($\text{Ru}(\text{bpy})_2\text{m})\text{-OH}](\text{PF}_6)_2$ ($^{\alpha}\text{N}$ -Boc-1**). Anal. Calcd for $\text{C}_{40}\text{H}_{40}\text{F}_{12}\text{N}_8\text{O}_5\text{P}_2\text{Ru}$: C, 43.53; H, 3.65; N, 10.15. Found: C, 43.86; H, 4.04; N, 9.86. UV–vis (MeOH) λ_{max} [nm] (ϵ , $[\text{M}^{-1} \text{cm}^{-1}]$): 455 (16 900), 288 (>50 000), 246 (30 600).**

[Bis(2,2'-bipyridine)(4-(carboxamido- $^{\alpha}\text{N}$ -($^{\alpha}\text{N}$ -1,1-dimethylethoxy-carbonyl-L-2,4-diaminobutyric acid))-4'-methyl-2,2'-bipyridyl)ruthenium(II)] Bis(hexafluorophosphate) [$^{\alpha}\text{N}$ -Boc-DABA($\text{Ru}(\text{bpy})_2\text{m})\text{-OH}](\text{PF}_6)_2$ ($^{\alpha}\text{N}$ -Boc-2**). Anal. Calcd for $\text{C}_{41}\text{H}_{42}\text{F}_{12}\text{N}_8\text{O}_5\text{P}_2\text{Ru}$: C, 44.05; H, 3.79; N, 10.02. Found: C, 44.20; H, 3.98; N, 9.84. UV–vis (MeOH) λ_{max} [nm] (ϵ , $[\text{M}^{-1} \text{cm}^{-1}]$): 455 (15 300), 288 (>50 000), 247 (28 600).**

[Bis(2,2'-bipyridine)(4-(carboxamido- $^{\alpha}\text{N}$ -($^{\alpha}\text{N}$ -1,1-dimethylethoxy-carbonyl-L-ornithine))-4'-methyl-2,2'-bipyridyl)ruthenium(II)] Bis(hexafluorophosphate) [$^{\alpha}\text{N}$ -Boc-Orn($\text{Ru}(\text{bpy})_2\text{m})\text{-OH}](\text{PF}_6)_2$ ($^{\alpha}\text{N}$ -Boc-3**). Anal. Calcd for $\text{C}_{42}\text{H}_{44}\text{F}_{12}\text{N}_8\text{O}_5\text{P}_2\text{Ru}$: C, 44.57; H, 3.92; N, 9.90. Found: C, 44.81; H, 4.11; N, 10.12. UV–vis (MeOH) λ_{max} [nm] (ϵ , $[\text{M}^{-1} \text{cm}^{-1}]$): 455 (15 100), 288 (>50 000), 247 (27 100).**

[Bis(2,2'-bipyridine)(4-(carboxamido- $^{\alpha}\text{N}$ -($^{\alpha}\text{N}$ -1,1-dimethylethoxy-carbonyl-L-lysine))-4'-methyl-2,2'-bipyridyl)ruthenium(II)] Bis(hexafluorophosphate) [$^{\alpha}\text{N}$ -Boc-Lys($\text{Ru}(\text{bpy})_2\text{m})\text{-OH}](\text{PF}_6)_2$ ($^{\alpha}\text{N}$ -Boc-4**). Anal. Calcd for $\text{C}_{43}\text{H}_{46}\text{F}_{12}\text{N}_8\text{O}_5\text{P}_2\text{Ru}$: C, 44.72; H, 4.10; N, 9.72. Found: C, 44.76; H, 4.31; N, 9.78. UV–vis (MeOH) λ_{max} [nm] (ϵ , $[\text{M}^{-1} \text{cm}^{-1}]$): 456 (14 800), 288 (>50 000), 245 (27 300).**

(20) Küster, F. W.; Thiel, A.; Ruland, A. *Rechentafeln für die chemische Analytik*, 103rd ed.; W. de Gruyter: Berlin, New York, 1985; p 161.

(21) Sullivan, B. P.; Salmon, D. J.; Meyer, T. J. *Inorg. Chem.* **1978**, *17*, 3334–3341.

(22) Peek, B. M.; Ross, G. T.; Edwards, S. W.; Meyer, G. J.; Meyer, T. J.; Erickson, B. W. *Int. J. Pept. Protein Res.* **1991**, *38*, 114–123.

(18) Alsfasser, R.; van Eldik, R. *Inorg. Chem.* **1996**, *35*, 628–636.

(19) Geißler, B.; Alsfasser, R. *Eur. J. Inorg. Chem.* **1998**, 957–963.

Table 2. Experimental Details for the Synthesis of **1–4**

product	[α -N ¹ -Boc-AA(Ru(bpy) ₂ m)-OH](PF ₆) ₂ mg (mmol)	yield mg (%)
1	400 (0.36)	240 (56)
2	400 (0.36)	324 (78)
3	300 (0.26)	186 (62)
4	400 (0.36)	310 (75)

Amino Acid Deprotection. The respective α -N-protected amino acid [α -N¹-Boc-AA(Ru(bpy)₂m)-OH](PF₆)₂ was stirred for 1 h at 0 °C in a mixture of 10 mL dioxane and 3 mL 4 N HCl. All solvent was removed by rotary evaporation, and the residue was dried in vacuo overnight. The obtained solid was dissolved in 50 mL of water, neutralized with 2 M NaOH, and purified by ion exchange chromatography (Sephadex CM-50) with a NaCl gradient in aqueous phosphate buffer (0.6 mM, pH = 7.2). A first band was obtained at 10 mM NaCl which contained traces of [Ru(bpy)₂(m-OH)]²⁺. The product eluted with 35 mM NaCl.

Rotary evaporation to dryness afforded an orange solid which was stirred for 30 min at room temperature (RT) in a minimum volume of acetonitrile/methanol (10:1, v/v). The red suspension was filtered to remove insoluble salt, all solvent was stripped by rotary evaporation, and the resulting red solid dried overnight under vacuum.

The crude products were dissolved in 10 mL of water, precipitated with a 1.5-fold excess of NH₄PF₆ in 1 mL of water, filtered, washed with 3 × 5 mL of water, and dried under vacuum. To obtain the complexes free of coprecipitated salts, they were suspended in 10 mL of water, sonicated for 30 min, and stirred for 24 h at RT. To yield the compounds in their fully protonated form, 250 μ L of 60% HPF₆ was added. The brown-orange precipitate was isolated by filtration, washed with 3 × 5 mL 1% HPF₆, and dried in a vacuum desiccator over silica gel. Yields based on protected amino acid complexes are summarized in Table 2.

[Bis(2,2'-bipyridine)(4-(carboxamido- β -N-L-2,3-diaminopropionic acid)-4'-methyl-2,2'-bipyridyl)ruthenium(II)] Tris(hexafluorophosphate) [H₃N-DAPA(Ru(bpy)₂m)-OH](PF₆)₃ (1**). Anal. Calcd for C₃₅H₃₃F₁₈N₈O₃P₃Ru·2H₂O: C, 35.46; H, 3.15; N, 9.45. Found: C, 35.75; H, 3.35; N, 9.26. UV-vis (H₂O) λ_{\max} [nm] (ϵ , [M⁻¹ cm⁻¹]): 457 (17 700), 287 (>50 000), 245 (32 700).**

[Bis(2,2'-bipyridine)(4-(carboxamido- γ -N-L-2,4-diaminobutyric acid)-4'-methyl-2,2'-bipyridyl)ruthenium(II)] Tris(hexafluorophosphate) [H₃N-DABA(Ru(bpy)₂m)-OH](PF₆)₃ (2**). Anal. Calcd for C₃₆H₃₅F₁₈N₈O₃P₃Ru·2H₂O: C, 36.04; H, 3.28; N, 9.34. Found: C, 35.89; H, 3.27; N, 9.04. UV-vis (H₂O) λ_{\max} [nm] (ϵ , [M⁻¹ cm⁻¹]): 457 (18 000), 287 (>50 000), 245 (34 400).**

[Bis(2,2'-bipyridine)(4-(carboxamido- δ -N-L-ornithine)-4'-methyl-2,2'-bipyridyl)ruthenium(II)] Tris(hexafluorophosphate) [H₃N-Orn(Ru(bpy)₂m)-OH](PF₆)₃ (3**). Anal. Calcd for C₃₇H₃₇F₁₈N₈O₃P₃Ru·H₂O: C, 37.17; H, 3.29; N, 9.37. Found: C, 37.04; H, 3.22; N, 9.12. UV-vis (H₂O) λ_{\max} [nm] (ϵ , [M⁻¹ cm⁻¹]): 457 (17 600), 287 (>50 000), 246 (34 300).**

[Bis(2,2'-bipyridine)(4-(carboxamido- ϵ -N-L-lysine)-4'-methyl-2,2'-bipyridyl)ruthenium(II)] Tris(hexafluorophosphate) [H₃N-Lys(Ru(bpy)₂m)-OH](PF₆)₃ (4**). Anal. Calcd for C₃₈H₃₉F₁₈N₈O₃P₃Ru·H₂O: C, 37.69; H, 3.41; N, 9.20. Found: C, 37.72; H, 3.52; N, 8.96. UV-vis (H₂O) λ_{\max} [nm] (ϵ , [M⁻¹ cm⁻¹]): 457 (17 600), 287 (>50 000), 245 (33 000).**

[Bis(2,2'-bipyridine)(4-N,N-diethylcarboxamido-4'-methyl-2,2'-bipyridine)ruthenium(II)] Bis(hexafluorophosphate) [Ru(bpy)₂(m-NEt₂)](PF₆)₂ (5**). Under nitrogen, 330 mg (0.33 mmol) [Ru(bpy)₂(m-OSu)](PF₆)₂ and 100 μ L (1.9 mmol) freshly distilled HNEt₂ were dissolved in 5 mL of DMF, and the dark-red mixture was stirred for 1.5 h at 41 °C. After the DMF and excess amine were removed by rotary evaporation, the orange solid was suspended in 100 mL of water and purified by ion exchange chromatography (Sephadex CM-50) with a NaCl gradient in aqueous phosphate buffer (0.6 mM, pH 7.2). The desired product was eluted as the second band with 35 mM NaCl. The solution was evaporated to dryness, and the resulting solid was dried in vacuo overnight.**

To remove excess salts, the red solid was stirred for 30 min at RT in a minimum volume of acetonitrile/methanol (5:1, v/v). After filtration,

all solvent was removed and the residue was dried in vacuo overnight. The crude product was dissolved in 10 mL of water and precipitated with a 1.5-fold excess of NH₄PF₆ in 1 mL of water. After the suspension was stirred at room temperature for 30 min, the orange precipitate was isolated by filtration, washed three times with 3 mL of water, and dried in a vacuum desiccator over silica gel (yield: 247 mg, 77%).

Anal. Calcd for C₃₆H₃₅F₁₂N₇OP₂Ru: C, 44.45; H, 3.63; N, 10.08. Found: C, 43.86; H, 3.55; N, 9.80. UV-vis (H₂O) λ_{\max} [nm] (ϵ , [M⁻¹ cm⁻¹]): 457 (15 300), 287 (>50 000), 245 (28 000).

Results

Synthesis and Characterization. Our synthesis of [Ru(bpy)₃]²⁺ modified amino acids followed the original preparation of [α -N¹-Boc-Lys(Ru(bpy)₂m)-OH]²⁺ (α -N¹-Boc-**4**) by Erickson et al.²² The succinimido ester [Ru(bpy)₂(m-OSu)](PF₆)₂ was reacted with the respective α -N¹-Boc-protected L-amino acid to afford the ruthenium-substituted α -N¹-Boc-derivatives of **1–4** (Figure 1) with over 90% yields. A number of photoredox active peptides^{5,22} and peptide analogues,^{23–25} as well as ruthenium-modified proteins^{4,7,26} containing the lysine derivative **4** have been reported earlier. However, little is known about the photophysical and chemical properties of the constituting ruthenium-modified amino acid itself. We therefore focused on the isolation, characterization, and purification of the deprotected amino acids **1–4** in order to investigate the dependence of their photophysical properties on side chain structures and pH effects.

Acid deprotection of α -N¹-Boc-(**1–4**) is easily achieved in dioxane/HCl. Ion exchange chromatography followed by precipitation of the ruthenium complexes with ammonium hexafluorophosphate was used for purification of the free amino acids. We found that it was difficult to remove excess salts which accumulated during chromatography (NaCl) and precipitation (NH₄PF₆). Analytically pure compounds were obtained only by repeated stirring of suspensions of the amino acid complexes in water followed by acidification with HPF₆. As a consequence of this workup, we always isolate the pure complexes in their +3 state with the amino acid carboxylate functions protonated. Losses during the purification process cause the yields to vary between 60% and 80% based on the protected ruthenated amino acids. Elemental analysis data indicate the presence of ca. 1 equiv of water which could not be removed by drying the compounds several days over silica gel under vacuum. The hexafluorophosphate salts are poorly soluble in water. However, concentrations below 0.1 mM can be obtained, and the compounds readily dissolve in 0.01 M aqueous NaCl solutions permitting studies on aqueous solutions.

Proton NMR spectroscopy is the most valuable tool for structural characterization of the modified amino acids. Formation of the amide link during the synthesis of α -N¹-Boc-**1–4** is accompanied by a characteristic low-field shift of the amino acid ω -CH₂ signals (ca. 0.5 ppm). For the diaminopropionic acid (DAPA) derivative α -N¹-Boc-**1**, a concomitant shift of the α CH signal from 4.04 to 4.39 ppm is also observed. Successful deprotection is evident from loss of the ¹Boc resonance at ca. 1.4 ppm.

(23) Mecklenburg, S. L.; McCafferty, D. G.; Schoonover, J. R.; Peek, B. M.; Erickson, B. W.; Meyer, T. J. *Inorg. Chem.* **1994**, *33*, 2974–2983.

(24) Mecklenburg, S. L.; Peek, B. M.; Schoonover, J. R.; McCafferty, D. G.; Wall, C. G.; Erickson, B. W.; Meyer, T. J. *J. Am. Chem. Soc.* **1993**, *115*, 5479–5495.

(25) Mecklenburg, S. L.; Peek, B. M.; Erickson, B. W.; Meyer, T. J. *J. Am. Chem. Soc.* **1991**, *113*, 8540–8542.

(26) Pan, L. P.; Durham, B.; Wolinska, J.; Millett, F. *Biochemistry* **1988**, *27*, 7180–7184.

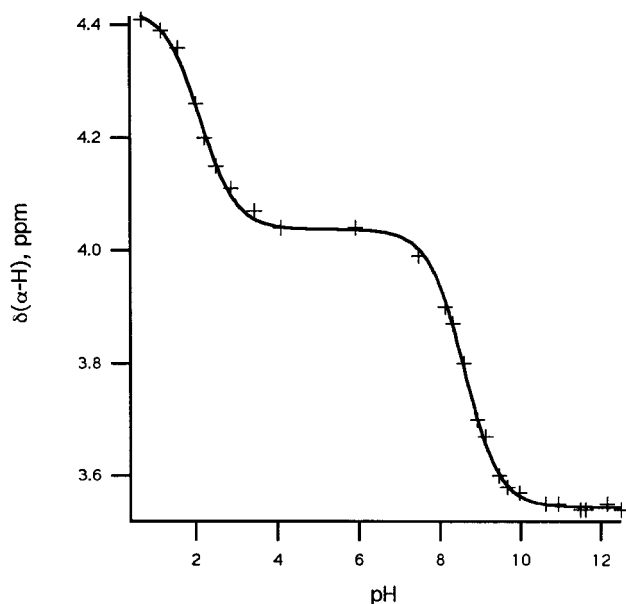


Figure 2. pH titration of **1** followed by NMR spectroscopy (chemical shift of the ^αCH group vs pH).

NMR Titrations. The ^αCH resonances of **1–4** are strongly pH dependent and shift to higher fields with increasing pH. This behavior is expected and typical for amino acids.^{27,28} The ground-state pK_A values of the amino acid functions of **1–4** were determined by plotting the chemical shifts of the ^αCH groups vs pH (D₂O) and fitting the data to a three-state acid–base equilibrium.²⁹ The titration curve obtained for **1** is shown as an example in Figure 2. It has been shown by other authors that pK_A values obtained in D₂O usually agree well with pK_A values observed in H₂O and that a correction for deuterium effects is not necessary.³⁰ The results are summarized in Table 3 together with some literature data.³¹

It is evident from Table 3 that the acidities of both the amino and the carboxylate functions in **1–4** increase as the distance between the amino acid moiety and amide link is getting shorter. A comparison of the pK_{COOH} and pK_{NH₃} values of **1–4** with tabulated values for the corresponding α,ω-diamino acids without ruthenium modification shows that the amino acid functions are significantly more basic in the metal complexes. The values obtained for **1** and **2** compare better with those reported for the ω-amido-α-amino acids Asn and Gln than with those for DAPA and DABA, respectively. As would be expected, the shift of pK_A values due to metal functionalization is most pronounced for the derivative with the shortest alkyl chain, **1**, and relatively small for complex **4** with the longest spacer.

Absorption and Emission Spectra. The UV–visible spectra of **1–4** in aqueous solution are indistinguishable and typical for polypyridyl ruthenium complexes. The most significant

feature is an MLCT band with a maximum at 457 nm (ε = 17 700 M⁻¹ cm⁻¹) and a shoulder at 427 nm. A strong intraligand π–π* band appears at 287 nm (ε > 50 000 M⁻¹ cm⁻¹). No significant spectral changes were observed at pH values varying from 0 to 14. In strongly acidic solutions (HCl_{conc}), the MLCT bands start to broaden and a shoulder at lower energies appears. This is shown in parts a and b of Figure 3 for the complexes **1** and *N,N*-diethylamide **5**, respectively. We have prepared **5** as a control, allowing comparison to distinguish contributions from the amide link and the amino acid functions in **1–4**.

In Figure 4, the uncorrected maximum emission intensities of **1–4** are plotted as a function of pH. The compounds contain three protonation sites, the amide link, the carboxylate function, and the amine function, respectively. Two protonation steps corresponding to protonations of the amide and the amine functions are clearly separated in each case. For **1** and **2**, poorly resolved additional steps appear at ca. pH 3 which have been assigned to protonation of the carboxylate functions. The relevant apparent excited-state pK_A^{*} values were determined by fitting the data to a three-state acid–base equilibrium for **3** and **4**, and to a four-state equilibrium for **1** and **2**.²⁹ Also shown in Figure 4 is the luminescence titration curve obtained for **5** (two-state acid–base equilibrium). A more detailed plot comparing fits to a three-state and a four-state equilibrium, respectively, for **1** and **2** is available as Supporting Information, Figure S2.

Britton Robinson buffers²⁰ have been used between pH 1.8 and 12 in order to keep the ionic strength constant at 0.1 M. Measurements of emission intensities at various ionic strengths were made at pH 6.8 in order to investigate possible effects of ionic strength at the higher acid or base concentrations. No significant changes of the luminescence intensities were found in a range between 0.1 and 5 M ionic strength (adjusted with NaClO₄). The data obtained for compound **5** are available as Supporting Information, Figure S3. Similar results were observed for **1–4**.

At very high and very low pH values, the emission intensities of **1–4** do not vary with amino acid structures and are similar to those of **5**. Below pH 1, the emission of all complexes is highly quenched and the luminescence of **1–4** becomes undetectable in strong acidic solutions (Figure 5). Since **1–4** show the same behavior as **5**, we assign the inflection at low pH³² (Table 3) to an acid–base equilibrium involving the amide link rather than to deprotonation of the remote carboxylic acid groups. The emission spectra of **1–4** exhibit no significant shift of the band maxima to lower energies as the pH is lowered to 0, but the nonradiative decay rates increase by an order of magnitude. A small residual emission band is observed for **5** in strongly acidic solution (Figure 6). This band is significantly shifted to lower energies.

An interesting structure dependence is found in an intermediate pH range between ca. 2 and 10. Inflection points around pH 9 are observed for **1–4**, respectively, with pK_{NH₃}^{*} (Table 3) values which are typical for the R–NH₃⁺ function of α-amino acids³¹ and close to the ground-state pK_{NH₃} values we obtained by NMR spectroscopy. Between pH 2 and 8, the emission intensities increase significantly with the number of methylene groups, *n* (Figure 1). These findings were confirmed by lifetime measurements at three different pH values (0.5, 4, and 14; Table 4). Only a small shift of the emission bands to lower energy

(27) Evans, C. A.; Rabenstein, D. L. *J. Am. Chem. Soc.* **1974**, *96*, 7312–7317.

(28) Sayer, T. L.; Rabenstein, D. L. *Can. J. Chem.* **1976**, *54*, 3392–3400.

(29)
$$I_{\text{obs}} = \frac{I_{\text{M}} + I_{\text{MH}}10^{(pK_2 - \text{pH})} + I_{\text{MH}_2}10^{(pK_1 + pK_2 - 2\text{pH})}}{1 + 10^{(pK_2 - \text{pH})} + 10^{(pK_1 + pK_2 - 2\text{pH})}}$$

For a complete treatment, refer to: Josceanu, A. M.; Moore, P.; Rawle, S. C.; Sheldon, P.; Smith, S. M. *Inorg. Chim. Acta* **1995**, *240*, 159–168.

(30) Scheller, K. H.; Scheller-Krattiger, V.; Martin, R. B. *J. Am. Chem. Soc.* **1981**, *103*, 6833–6839.

(31) Kiss, T. In *Biocoordination Chemistry*; Burger, K., Ed.; Ellis Horwood: New York, 1990; pp 56–134.

(32) As one of the referees pointed out, the inflection point is no accurate measure for pK_A^{*} since the amide quenching is kinetically, rather than thermodynamically, controlled.

Table 3. Ground-State and Apparent Excited-State pK_A Values for **1–5** Determined by NMR and Luminescence Spectroscopy, Respectively, and Some Selected pK_A (Amino Acid– NH_3^+) Data³¹

compd	pK_{Amide}^* ^a	pK_{COOH}	pK_{COOH}^*	pK_{NH_3}	$pK_{NH_3}^*$
1	0.37 ± 0.04	2.14 ± 0.03	3.19 ± 0.80	8.59 ± 0.02	8.82 ± 0.05
2	0.37 ± 0.04	2.14 ± 0.04	2.81 ± 0.52	9.33 ± 0.02	9.37 ± 0.09
3	0.49 ± 0.02	2.29 ± 0.04		9.64 ± 0.02	10.21 ± 0.19
4	0.60 ± 0.02	2.31 ± 0.05		9.80 ± 0.03	10.10 ± 0.51
DAPA ³¹		1.3		6.68	
DABA ³¹		1.7		8.19	
Orn ³¹		1.9		8.78	
Lys ³¹		2.19		9.12	
Asn ³¹		2.15		8.72	
Gln ³¹		2.16		9.01	
5	0.31 ± 0.02				

^a Reported is the first inflection point of the curves shown in Figure 4.³²

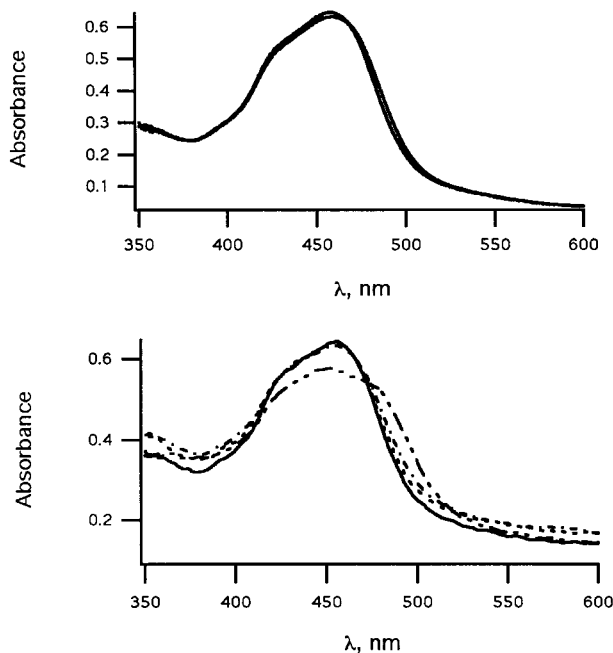


Figure 3. (a) MLCT bands of **1** (a) and **5** (b) at pH 12 (—), 0 (---), –0.78 (–·–), and –1.1 (····).

with decreasing intensities is observed at pH 4.75 consistent with the small differences between the ground-state pK_{NH_3} and the apparent excited-state $pK_{NH_3}^*$ values (Figure 5). Effects of the carboxylate functions on the luminescence properties cannot be quantified because they are only observable for **1** and **2** and largely obscured by the spectral changes due to amide protonation.

Discussion. The pH-dependent emission properties of the *N,N*-diethylamide **5** resemble those of $[Ru(bpy)_3]^{2+}$ derivatives bearing carboxylate groups directly attached to one or more of the bipyridine ligands. These compounds have found considerable interest as sensitizers for water splitting devices^{33–36} and luminescent probes for binding studies on microparticles such as micelles,³⁷ and their photophysical properties have therefore been studied in much detail.³⁸ In general, protonation of a

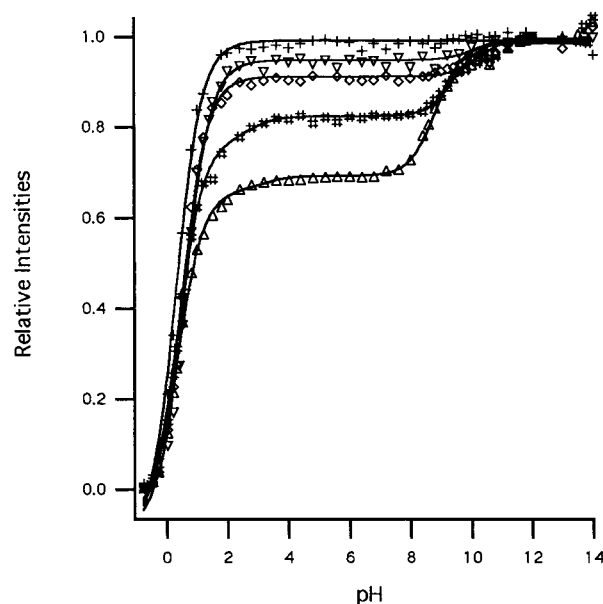


Figure 4. pH dependence of the maximum emission intensities of **1** (Δ), **2** ($\#$), **3** (\diamond), **4** (∇), and **5** ($+$) (intensities are relative to the values measured at pH 12; $\lambda_{exc} = 450$ nm).

functional group in conjugation with the bipyridine ligand leads to luminescence quenching (Scheme 1). The ground-state pK_A 's of the carboxylate groups on $[Ru(bpy)_2(4,4'\text{-dcbpy})]^{2+}$ are 2.15 and 1.75, respectively, resulting in pH-dependent UV–vis spectra.^{39–44} The emission spectra are also pH dependent, with an apparent excited-state pK_A^* of 4.25. The difference between ground- and excited-state pK_A 's indicates increased basicity of the excited state with respect to the ground state.

We interpret the pH-dependent emission behavior of **5** as the result of an amide oxygen protonation in the excited state. Quenching at low pH is considerably more efficient in our amide complex than in corresponding carboxylate species and occurs at higher $[H^+]$. The UV–vis spectrum of the complex is pH independent in the pH = 0–14 range. A shift of the MLCT bands to lower energies is observed in strongly acidic solutions

(33) Desilvestro, J.; Grätzel, M.; Kavan, L.; Moser, J. *J. Am. Chem. Soc.* **1985**, *107*, 2988–2990.

(34) Furlong, D. N.; Wells, D.; Sasse, W. H. F. *J. Phys. Chem.* **1986**, *90*, 1107–1115.

(35) Dabestani, R.; Bard, A. J.; Campion, A.; Fox, M. A.; Mallouk, T. E.; Webber, S. E.; White, J. M. *J. Phys. Chem.* **1988**, *92*, 1872–1878.

(36) Vlachopoulos, N.; Liska, P.; Augustynski, J.; Grätzel, M. *J. Am. Chem. Soc.* **1988**, *110*, 1216–1220.

(37) Foreman, T. K.; Sobol, W. M.; Whitten, D. G. *J. Am. Chem. Soc.* **1981**, *103*, 5333–5336.

(38) Vos, J. G. *Polyhedron* **1992**, *11*, 2285–2299.

(39) Giordano, P. J.; Bock, C. R.; Wrighton, M. S.; Interrante, L. V.; Williams, R. F. X. *J. Am. Chem. Soc.* **1977**, *99*, 3187–3195.

(40) Lay, P. A.; Sasse, W. H. F. *Inorg. Chem.* **1984**, *23*, 4123–4125.

(41) Nazeeruddin, M. K.; Kalyanasundaram, K. *Inorg. Chem.* **1989**, *28*, 4251–4259.

(42) Shimidzu, T.; Iyoda, T.; Izaki, K. *J. Phys. Chem.* **1985**, *89*, 642–645.

(43) Kalyanasundaram, K.; Nazeeruddin, M. K.; Grätzel, M. *Inorg. Chim. Acta* **1992**, *198–200*, 831–839.

(44) Park, J. W.; Ahn, J.; Lee, C. *J. Photochem. Photobiol. A* **1995**, *86*, 89–95.

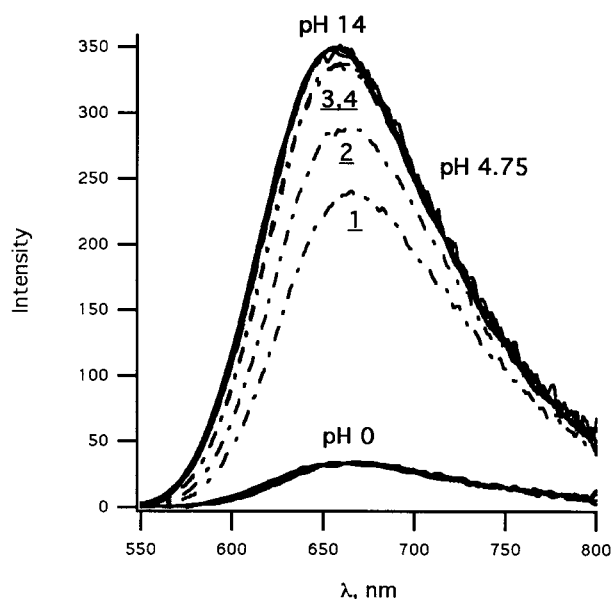


Figure 5. Luminescence spectra of **1–4** at pH = 14 (highest intensities; indistinguishable within the experimental error), pH = 4.75 (---; compounds indicated; intensities decrease with the number of methylene spacers), and pH = 0 (lowest intensities; indistinguishable within the experimental error).

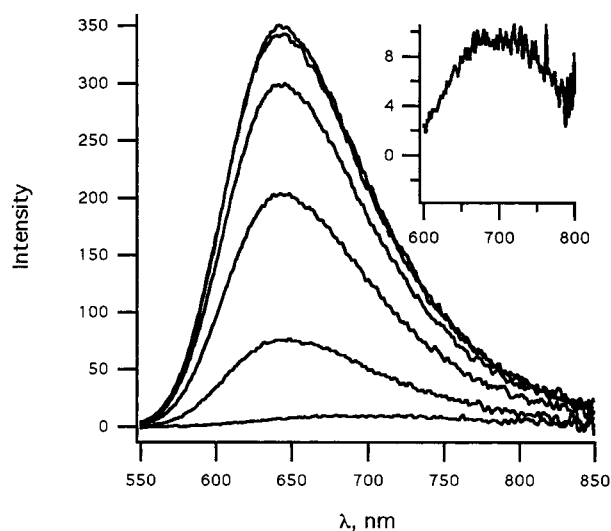


Figure 6. Luminescence spectra of **5** at pH = 14, 2, 1, 0.5, 0, and -1.1 (decreasing intensities). Inset: spectrum at pH -1.1.

(pH < -1; Figure 3), indicating that the ground-state pK_A values of the amide oxygen is below 0. Although the difference between ground- and excited-state pK_A is not quantified, the excited state is expected to be more basic than the ground state since three mesomeric structures exist in the excited state in which the amide oxygen carries a partial negative charge. (Figure 7).⁴⁵

The amino acid complexes **1–4** also show efficient luminescence quenching at pH values below 1, which is mainly due to protonation of the amide links. A small superimposed effect of the carboxylate functions in **1** and **2** is evident from the titration curves shown in Figure 4. The absorption spectra of **1–4** do not change with either pH or side chain structure, indicating the absence of direct electronic interactions between the amino acid functions and the ruthenium chromophore. This behavior is expected since the methylene spacers prevent efficient electronic coupling between the two functional groups.

No significant shift of the emission bands to lower energies is observed as the pH is lowered to 0, but the nonradiative decay rates increase significantly. This observation is consistent with the presence of an excited-state quenching mechanism by proton transfer according to general kinetic Scheme 1.¹⁶

The luminescence of *M is quenched by protons according to the Stern–Volmer relationship given in eqs 1 and 2.

$$\frac{\tau_0}{\tau} = 1 + \frac{k_H \tau_0}{1 + k_{-H} \tau_0} [\text{H}^+] = 1 + k_q \tau_0 [\text{H}^+] \quad (1)$$

$$k_q = \frac{k_H}{1 + k_{-H} \tau_0} \quad (2)$$

If the protonated complex $^*MH^+$ in Scheme 1 is very short lived ($\tau_0 \gg \tau_0'$) emission is predominantly observed from *M . In such a case, one would not expect the emission band to shift significantly upon lowering the pH. It is evident from Figure 4 that the titration curve has not reached its minimum at pH 0. Thus, *M (unprotonated amide link) will contribute significantly to the observed luminescence explaining the negligible red shift of the emission curve maxima. At pH values below 0, the emission of **1–4** is undetectable. For complex **5**, a residual emission is observed at pH -1.1 (Figure 6) and the band appears significantly shifted to lower energies. A plot of the emission lifetimes of **5** vs $[\text{H}^+]$ shows the expected linear Stern–Volmer behavior in a pH range between 3 and -0.5 (Figure 8). In this range, no significant band shift is observed. In 12 M HCl solution, the steady-state approximation leading to eq 1 does not any longer hold and emission of the protonated complex is observed. This is evident from the expected low-energy shift of the emission band.

It is evident from our data that the remote amino acid moiety has an effect on the excited-state properties of the amino acid complexes in a pH range between ca. 2 and 10 (Figure 4). The observed shift of emission energies along the series **1–4** (Table 4, Figure 5) indicates a smaller separation of ground and excited states in **1** and **2**. This could contribute to the observed increase in nonradiative decay rates according to the energy gap law.^{46,47} The effect is small, and the inflection points observed by luminescence titrations are close to the ground-state pK_A values of the amino acid NH_3^+ groups. Contributions of the carboxylate functions to nonradiative decay processes are largely obscured by the amide protonation at low pH. However, the titration curves obtained for **1** and **2** indicate that carboxylate protonation also leads to enhanced nonradiative decay rates.

No significant coupling of the amino acid functions of **1–4** to the chromophore is observed in the ground state and it is surprising to find a significant effect of the protonation state of this group on the luminescence spectra. It is therefore likely that weak intramolecular interactions such as hydrogen bonding between the remote functional group and the chromophore contribute to the excited-state dynamics of our molecules. Intermolecular hydrogen bonding interactions between amide bonds and anions such as Cl^- , Br^- , and I^- have been discussed as being the basis for anion recognition sensors based on polypyridyl ruthenium complexes.^{48–50} Further investigations

(45) Ford, W. E.; Calvin, M. *Chem. Phys. Lett.* **1980**, *76*, 105–108.

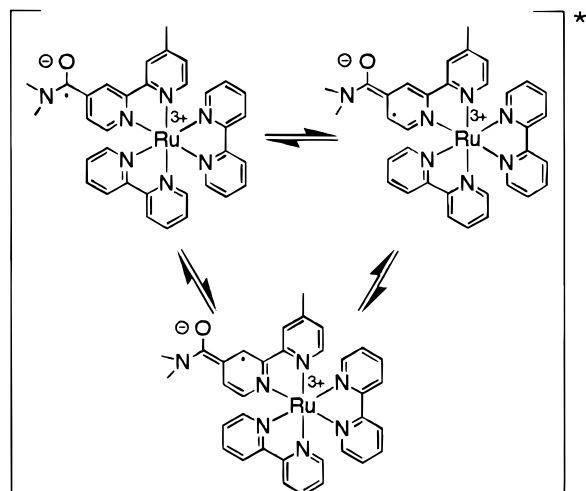
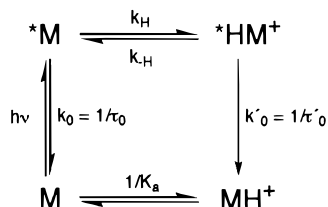
(46) Turro, N. J. *Modern Molecular Photochemistry*; Benjamin Cummings: Menlo Park, CA, 1978.

(47) Caspar, J. V.; Kober, E. M.; Sullivan, B. P.; Meyer, T. J. *J. Am. Chem. Soc.* **1982**, *104*, 630–632.

(48) Beer, P. D.; Dent, S. W.; Wear, T. J. *J. Chem. Soc., Dalton Trans.* **1996**, 2341–2346.

Table 4. Excited-State Lifetimes and Emission Energies of **1–4** at Different pH Values

compd	pH = 0		pH = 4.75		pH = 14	
	τ , ns	E_{em} , cm ⁻¹	τ , ns	E_{em} , cm ⁻¹	τ , ns	E_{em} , cm ⁻¹
1	64 ± 1	14880	337 ± 3	14970	429 ± 4	15174
2	77 ± 1	14880	386 ± 3	15060	412 ± 4	15174
3	61 ± 1	14880	420 ± 4	15128	444 ± 4	15174
4	59 ± 1	14880	427 ± 4	15151	412 ± 4	15174

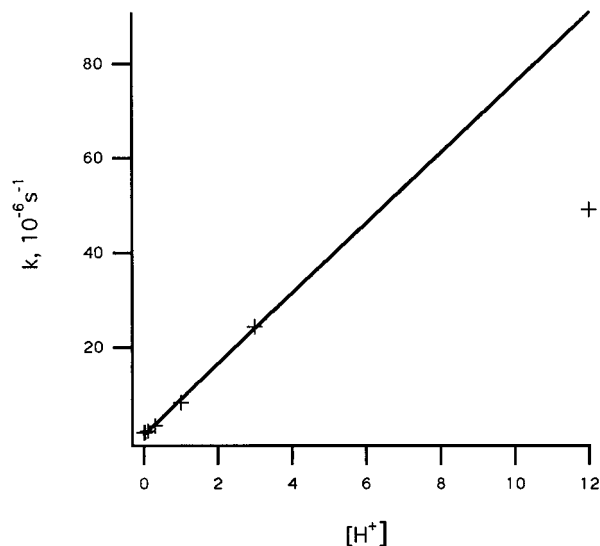
**Figure 7.** Mesomeric excited-state structures with a negative charge on the amide oxygen in **1–4**.**Scheme 1.** Ground- and Excited-State Acid–Base Equilibria

such as quenching experiments with carboxylate anions and ammonium cations as well as resonance Raman studies are currently underway and will focus on the mechanisms involved.

It is interesting to note that we did not find evidence for any specific solvent–solute interactions. This may be surprising since solvation effects have been discussed to be important in determining the emission properties of ruthenium complexes in aqueous solution⁵¹ and other polar solvents.¹⁴ It has been reported that the solvent reorganization energy term χ may significantly contribute to the excited-state decay of transition metal chromophores in aqueous medium.^{12,13,52} Changes in χ should be reflected by changes of the emission band line widths since these properties are connected through eq 3.⁵¹

$$\chi = \frac{(\Delta\nu_{1/2})^2}{(16k_B T \ln 2)} \quad (3)$$

However, we do not observe significant changes in line widths at different pH values or for different amino acid structures in **1–4**. Thus, different reorganization energies as a consequence

**Figure 8.** Plot of $1/\tau$ vs $[H^+]$.

of varying solvation spheres are unlikely to explain the observed pH-dependent emission behavior.

Conclusions

The results presented in this report show that large perturbations of excited-state dynamics of ruthenium tris(bipyridine) can result when subtle changes of remote functional groups are effected. The systems we studied are particularly relevant for sensing applications of luminescent metal complexes in biological systems since the amide link used for the synthesis of **1–4** provides a convenient route to metalated peptides and proteins. Our data suggest that this linkage can be subject to changes in the microenvironment controlling the photophysical properties of the chromophore used. This is important since it demonstrates how the choice of coupling methods can have an impact on experimental results by changing the properties of the chromophores used.

The modulation of excited-state energetics by weak intramolecular interactions between the chromophore and remote functional groups provides an interesting means of controlling the properties of supramolecular photochemical molecular devices (PMDs).⁵³ It supplements the tuning of photoredox properties by ligand modification.^{54–56}

Acknowledgment. The authors gratefully acknowledge financial support from the Deutsche Volkswagenstiftung and

- (49) Beer, P. D.; Dent, S. W.; Fletcher, N. C.; Wear, T. J. *Polyhedron* **1996**, *15*, 2983–2996.
 (50) Beer, P. D. *Chem. Commun.* **1996**, 689–696.
 (51) Caspar, J. V.; Sullivan, B. P.; Kober, E. M.; Meyer, T. J. *Chem. Phys. Lett.* **1982**, *91*, 91–95.
 (52) Murtaza, Z.; Graff, D. K.; Zipp, A. P.; Worl, L. A.; Jones, W. E.; Bates, W. D.; Meyer, T. J. *J. Phys. Chem.* **1994**, *98*, 10504–10513.

- (53) Balzani, V.; Scandola, F. In *Supramolecular Technology*; Reinholdt, D. N., Ed.; Elsevier: Oxford, 1996; Vol. 10; pp 687–746.
 (54) Furue, M.; Maruyama, K.; Oguni, T.; Naiki, M.; Kamachi, M. *Inorg. Chem.* **1992**, *31*, 3792–3795.
 (55) Maestri, M.; Armaroli, N.; Balzani, V.; Constable, E. C.; Cargill Thompson, A. M. W. *Inorg. Chem.* **1995**, *34*, 2759–2767.
 (56) Anderson, P. A.; Deacon, G. B.; Haarmann, K. H.; Keene, F. R.; Meyer, T. J.; Reitsma, D.; Skelton, B. W.; Strouse, G. F.; Thomas, N. C.; Treadway, J. A.; White, A. H. *Inorg. Chem.* **1995**, *34*, 6145–6157.

the Deutsche Forschungsgemeinschaft (Habilitationstipendium for R.A.). We thank Prof. H. B. Gray and Dr. J. R. Winkler for their support, and Prof. G. Löhmansröben for helpful discussions. This work would not have been possible without the support of Prof. Rudi van Eldik who generously let us share his equipment, laboratory space, and funding.

Supporting Information Available: Listings of NMR, IR, and C,H,N analytical data for all complexes, as well as two figures showing emission titration data for **1** and **2** and ionic strength dependent luminescence intensities of **5**, respectively. This material is available free of charge via the Internet at <http://pubs.acs.org>.

IC980896X